

## Experimental observation of the dual behavior of $\mathcal{PT}$ -symmetric scattering

Zin Lin, Joseph Schindler, Fred M. Ellis, and Tsampikos Kottos

*Department of Physics, Wesleyan University, Middletown, Connecticut 06459, USA*

(Received 25 February 2012; published 4 May 2012)

We investigate experimentally parity-time ( $\mathcal{PT}$ ) symmetric scattering using  $LRC$  circuits in an inductively coupled  $\mathcal{PT}$ -symmetric pair connected to transmission line leads. In the single-lead case, the  $\mathcal{PT}$ -symmetric circuit acts as a simple dual device—an amplifier or an absorber depending on the orientation of the lead. When a second lead is attached, the system exhibits unidirectional transparency for some characteristic frequencies. This nonreciprocal behavior is a consequence of generalized (nonunitary) conservation relations satisfied by the scattering matrix.

DOI: [10.1103/PhysRevA.85.050101](https://doi.org/10.1103/PhysRevA.85.050101)

PACS number(s): 11.30.Er, 03.65.Nk, 05.60.–k

While there is absolutely no doubt as to the usefulness of gain mechanisms for signal boosting and information transfer, loss, on the other hand, is typically undesirable—one to be avoided if at all possible—since it degrades the efficiency of the structures employed to perform useful operations on these signals. It is perhaps for this reason that researchers have never intentionally explored the combination of gain and loss as a duality of useful ingredients in device and materials engineering.

Currently, however, an alternate viewpoint is emerging aiming to manipulate absorption, and, via a judicious design that involves the combination of delicately balanced amplification and absorption mechanisms, achieve classes of synthetic structures with altogether new physical behavior and novel functionality. This idea deliberately exploits notions of parity ( $\mathcal{P}$ ) and time ( $\mathcal{T}$ ) symmetry [1–3] and can be naturally incorporated into the framework of classical optics [4]. In fact, optical media with delicately balanced gain and loss characteristics of systems with joint parity-time ( $\mathcal{PT}$ ) symmetry have been reported [5] showing several intriguing features [4–21]. These include, among others, power oscillations and nonreciprocity of light propagation [4,5,10], nonreciprocal Bloch oscillations [11], and unidirectional invisibility [19]. In the nonlinear domain, such pseudo-Hermitian nonreciprocal effects can be used to realize a new generation of on-chip isolators and circulators [9]. Other results within the framework of  $\mathcal{PT}$ -optics include the realization of coherent perfect laser-absorber [13,14] and nonlinear switching structures [15].

More recently these ideas have been extended into the realm of electronic circuitry [22], where it was demonstrated that a pair of coupled  $LRC$  circuits, one with amplification and the other with an equivalent amount of attenuation, provide the simplest experimental realization of a  $\mathcal{PT}$ -symmetric system. The  $\mathcal{PT}$ -circuitry approach suggested in Ref. [22] opens new avenues for innovative integrated circuitry architectures which will afford novel avenues for signal manipulation, and reduced circuit loss. Moreover, it allows for direct contact with cutting edge technological problems appearing in (nano)antenna theory and split-ring resonator metamaterial arrays.

Although the study of  $\mathcal{PT}$ -symmetric Hamiltonians has been a subject of intense research efforts, relatively few authors have up to now theoretically studied the equivalent scattering system [12–14,16–19,23]. Given that the additional freedom of the gain and loss parameter will lead to a wealth of novel

scattering phenomena, it is surprising that there is a lack of experimental investigations on  $\mathcal{PT}$  scattering.

Here we report initial experimental results for the scattering properties of  $\mathcal{PT}$ -symmetric systems. The scattering setup consists of a pair of inductively coupled  $LRC$  oscillators, one with gain and the other with loss, coupled to transmission line (TL) leads. Our measurements reveal the signatures of the parity-time symmetry in the conservation relations satisfied by the nonunitary scattering matrix. In the simplest possible scattering setup where the target is coupled to a single TL, we find that the reflection signal is nonreciprocal and respects the (nonunimodular) conservation relation  $r_L r_R^* = 1$ , where  $r_L(r_R)$  is the reflection associated to a left (right) incident wave. Furthermore, we have identified a transition from a subunitary to a superunitary scattering process and associate it with the spatial structure of the potential inside the scattering domain. Once a second TL is attached to the  $\mathcal{PT}$  scatterer, the system demonstrates unidirectional transparency, where the transmittance is unity and the reflectance is zero, but only for waves incident from a single side. Being free of basic theoretical approximations, and due to its relative simplicity in the experimental implementation, the  $LRC$  networks with  $\mathcal{PT}$  symmetry can offer unique insights into the study of  $\mathcal{PT}$ -symmetric scattering which is at the forefront of current research in various areas of physics.

The heart of the  $\mathcal{PT}$ -symmetric scatterer (load) is the pair of inductively coupled  $LC$  resonators (dimer) shown in the insets of Fig. 1 [22]. Each inductor consists of 75 turns of #24 copper wire wound on 15-cm-diam polyvinyl chloride (PVC) forms in a  $6 \times 6$  mm loose bundle for an inductance  $L_0 = 2.32$  mH. The coils, matched to within 1% by repositioning one of the turns, are mounted coaxially with a bundle separation that determines the mutual coupling of  $\mu = M/L_0 = 0.29$  used for the data presented in this work. The capacitances are 10.36 nF silver mica in addition to the self-capacitance of the coil bundles of  $\sim 320$  pF. Capacitance balance is trimmed by substituting  $\sim 360$  pF of one side with a GR722-M variable capacitance. The uncoupled frequency of each resonator is  $\omega_0 = 1/\sqrt{LC} = 2\pi\nu$  with  $\nu = 30.957$  kHz. Loss imposed on the right half of the dimer is a standard carbon resistor  $R$ . Gain imposed on the left half of the dimer, symbolized by  $-R$ , is implemented with an LF356-based negative impedance converter (NIC). The NIC gain is trimmed to oppositely match the value of  $R$  used on the loss side, setting the gain and loss

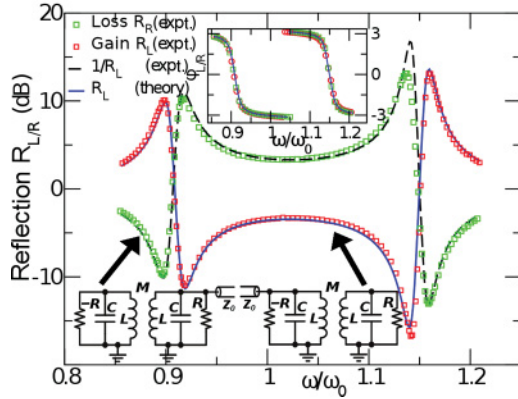


FIG. 1. (Color online) Experimental reflectances for a single TL attached to the lossy ( $R_R$ ) or the gain ( $R_L$ ) side of the dimer (see lower insets) for  $\mu = 0.29$ ,  $\gamma = 0.188875$ , and  $\eta = 0.0305$ . The black line corresponds to  $R_L^{-1}$  and confirms the nonreciprocal nature  $R_L R_R = 1$  of the  $\mathcal{PT}$  scattering. The upper inset shows the measurements for the left (right) reflection phases  $\phi_L$  ( $\phi_R$ ). The blue (dark gray) lines are the theoretical results, Eq. (4).

parameter  $\gamma = R^{-1}\sqrt{L/C} = 1/(\omega_0 RC)$ . An additional NIC is included on the loss side so that intrinsic resonator losses on both sides can be compensated for prior to setting the gain and loss parameter.

We start our scattering studies with the following two reciprocal geometries: In the first case, a TL is attached to the left (amplified) circuit of the dimer load while in the second case, the TL is connected to the right (lossy) circuit of the load (see lower right and left insets of Fig. 1, respectively). Experimentally, the equivalent of a TL with characteristic impedance  $Z_0$  is attached to either side of the dimer at the  $LC$  circuit voltage node in the form of a resistance  $R_0 = Z_0$  in series with an HP3325A synthesizer. The right and left traveling-wave components associated with the TL are deduced from the complex voltages on both sides of  $R_0$  with an EG&G 7256 lock-in amplifier. With  $V_{LC}$  the voltage on the  $LC$  circuit, and  $V_0$  the voltage on the synthesizer side of the coupling resistor  $R_0$ , the right (incoming) wave has a voltage amplitude  $V_L^+ = V_0/2$  and the left (reflected) wave has a voltage amplitude  $V_L^- = V_{LC} - V_0/2$ . The lock-in is referenced to the synthesizer, defining the phases of the wave components relative to the incoming wave.

At any point along a TL, the current and voltage determine the amplitudes of the right and left traveling-wave components [24]. The forward  $V_{L|R}^+$  and backward  $V_{L|R}^-$  wave amplitudes, and  $V_{L|R}$  and  $I_{L|R}$  the voltage and current at the left ( $L$ ) or right ( $R$ ) TL-dimer contacts satisfy the continuity relation

$$V_{L|R} = V_{L|R}^+ + V_{L|R}^-, \quad I_{L|R} = [V_{L|R}^+ - V_{L|R}^-]/Z_0, \quad (1)$$

which connects the wave components to the currents and voltages at the TL-dimer contact points. Note that with this convention, a positive lead current flows into the right circuit, but out of the left circuit, and that the reflection amplitudes for left or right incident waves are defined as  $r_L \equiv V_L^-/V_L^+$  and  $r_R \equiv V_R^+/V_R^-$ , respectively.

Application of the first and second Kirchoff's laws at the TL leads allows us to find the corresponding wave amplitudes and reflection. For example, the case of the left-attached lead

in the lower right inset of Fig. 1 gives

$$\begin{aligned} \eta(V_L^+ - V_L^-) &= I_L^M - \gamma V_L - i\omega V_L, \\ V_L &= -i\omega[I_L^M + \mu I_R^M], \quad V_R = -i\omega[I_R^M + \mu I_L^M], \\ 0 &= I_R^M + \gamma V_R - i\omega V_R, \end{aligned} \quad (2)$$

where  $\gamma$  is the gain and loss parameter,  $\eta = \sqrt{L/C}/Z_0$  is the dimensionless TL impedance, and  $I_{L|R}^M$  are the current amplitudes in the left or right inductors. Here, the dimensionless wave frequency  $\omega$  is in units of  $1/\sqrt{LC}$ . Similar equations apply for the right-attached case shown in the lower left inset of Fig. 1.

We are interested in the behavior of the reflectance  $R_{L|R} \equiv |r_{L|R}|^2$ , and spatial profile of the potential  $V_{L|R}$  inside the scattering domain, as the gain and loss parameter  $\gamma$  and the frequency  $\omega$  changes.

For  $\mathcal{PT}$ -symmetric structures, the corresponding scattering signals satisfy *generalized unitarity relations* which reveal the symmetries of the scattering target. Specifically, in the single-port setup this information is encoded solely in the reflection. To unveil it, we observe that the lower left setup of Fig. 1 is the  $\mathcal{PT}$ -symmetric replica of the lower right one. Assuming therefore that a potential wave at the left lead (lower right inset) has the form  $V_L(x) = \exp(ikx) + r_L \exp(-ikx)$  [we assume  $V_L^+ = 1$  and  $V_L^- = r_L$  in Eq. (1)], we conclude that the form of the wave at the right lead associated with the lower left setup of Fig. 1 is  $V_R(x) = \exp(-ikx) + r_r \exp(ikx) = V_L^*(-x)$ . Direct comparison leads to the relation

$$r_L r_R^* = 1 \rightarrow R_L = 1/R_R \quad \text{and} \quad \phi_L = \phi_R, \quad (3)$$

where  $\phi_L$  ( $\phi_R$ ) are the left (right) reflection phases. Note that Eq. (3) differs from the more familiar conservation relation  $R = 1$ , which applies to unitary scattering processes as a result of flux conservation. In the latter case the left and right reflectances are equal. Instead in the  $\mathcal{PT}$ -symmetric case we have in general that  $R_L \neq R_R$ .

For the specific case of the  $\mathcal{PT}$ -symmetric dimer, we can further calculate analytically the exact expression for the reflection coefficients. From Eqs. (2) we have

$$\begin{aligned} r_L(\omega) &= -f(-\eta, -\gamma)/f(\eta, -\gamma), \\ r_R(\omega) &= -f(-\eta, \gamma)/f(\eta, \gamma), \\ f &= 1 - [2 - \gamma m(\gamma + \eta)]\omega^2 + m\omega^4 - i\eta\omega(1 - m\omega^2), \end{aligned} \quad (4)$$

with

$$m = 1/\sqrt{1 - \mu^2}.$$

In the limiting case of  $\omega \rightarrow 0, \infty$  the reflections becomes  $r_R \rightarrow \mp 1$  and thus unitarity is restored.

In the main panel of Fig. 1 we report representative measurements of the reflection signals for the two scattering configurations and compare them with Eq. (4). The synthesizer frequency is slowly swept through the region of interest, producing the reflectance  $R_L = |V_L^-/V_L^+|$  as a function of frequency, resulting in the red (dark gray) squares of Fig. 1. A similar procedure is used to obtain the reflectance  $R_R$  from the right (loss) side of the dimer, resulting in the green (light gray) squares of Fig. 1. The measured reflectances  $R_L$  and  $R_R$  satisfy the generalized conservation relation  $R_L R_R = 1$  [25] while for the reflection phases we have that  $\phi_L = \phi_R$ , as expected

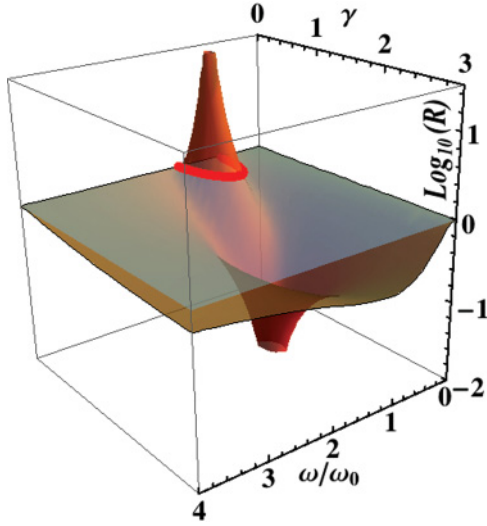


FIG. 2. (Color online) The  $\omega$ - $\gamma$  phase diagram for  $\mu = 0.57$ , indicating the existence of a subunitary [ $\log_{10}(R_R) < 0$ ] and a complimentary superunitary [ $\log_{10}(R_R) > 0$ ] domain for the setup shown at the lower left inset of Fig. 1; the (white) plane  $\log_{10}(R) = 0$  is shown for reference while the boundary Eq. (5) is indicated with a bold (red/gray) line.

from Eq. (3). Therefore, our experiment demonstrates that a  $\mathcal{PT}$ -symmetric load is a simple electronic dual device that for the same values of the parameters  $\omega, \mu, \gamma$  acts as an absorber as well as a signal amplifier, depending on the direction of the incident signal.

Next, we identify the existence of a *subunitary* domain for which  $R < 1$  (flux is diminished), and a *superunitary* domain for which  $R > 1$  (flux is enhanced). At the transition between the two domains  $R_L = R_R = 1$ , in which case the scattering from both sides conserves flux. Such *reflectance degeneracies* (RDs) occur as a parameter such as the frequency  $\omega$  (or  $\gamma$ ) is varied continuously. Requiring that  $|r_R| = 1$ , we get

$$\gamma^* = \sqrt{\frac{-1 + 2\omega^2 - (1 - \mu^2)\omega^4}{(1 - \mu^2)\omega^2}} \quad \text{and} \quad \frac{|\omega^2 - 1|}{\omega^2} \leq \mu \leq 1. \quad (5)$$

A panorama of theoretical  $R_R(\omega, \gamma)$  is shown in Fig. 2. In the same plot we mark the transition line  $\gamma^*(\omega)$  where a RD occurs. Inside this domain, a singularity point appears for which  $R_R \rightarrow \infty$ , while a reciprocal point for which  $R_R = 0$  is found in the complementary domain. The corresponding  $(\omega_s; \gamma_{\infty,0})$  are found from Eq. (4) to be  $\gamma_{\infty,0} = \frac{1}{2}(\sqrt{\eta^2 + \frac{4\mu^2}{(1-\mu^2)}} \mp \eta)$ ,  $\omega_s = \frac{1}{\sqrt{1-\mu^2}}$ . Obviously via Eq. (3) we have the reverse scenario for  $R_L$ .

The subunitary-to-superunitary  $\mathcal{PT}$ -symmetric transition is also manifest in the spatial structure of the potential  $(V_L; V_R)$  inside the dimer. From Eq. (2) we get

$$\begin{aligned} V_L &= 2\eta\omega[1 - m\omega(\omega - i\gamma)]/D, \\ V_R &= -2\eta\mu\omega/D, \\ D &= \eta\omega(1 - m\omega^2) + i\{1 - \omega^2[2 - m(\omega^2 + \gamma\omega + \gamma^2)]\}. \end{aligned} \quad (6)$$

Typical potential amplitudes  $(|V_L|; |V_R|)$  for the setup of the lower left inset of Fig. 1 versus the frequency  $\omega$  are shown

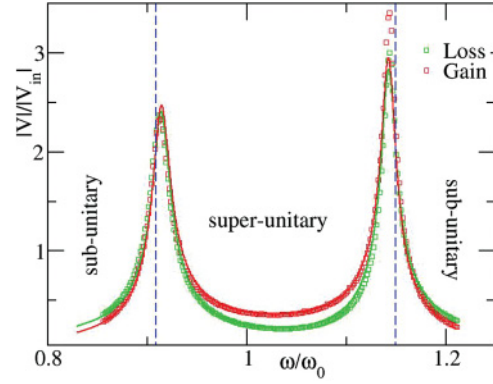


FIG. 3. (Color online) The spatial potential distribution inside the dimer versus the frequency  $\omega$ . The symbols correspond to experimental data while the lines to the theoretical predictions of Eq. (6). The TL is coupled to the lossy side. We have used the same parameters as those used in Fig. 1. The blue dashed lines indicate the boundaries between subunitary to superunitary scattering where RDs occur.

in Fig. 3. We observe that they are in general asymmetric. In the superunitary domain, the gain side is characterized by a larger potential amplitude  $|V_L| > |V_R|$  while in the subunitary domain the scenario is reversed and  $|V_L| < |V_R|$ . The latter configuration ensures that more power is being consumed than compensated for by the gain circuit, while the inverse argument applies for the former configuration. At frequencies where the RD occurs, the potential profiles are spatially symmetric. This is consistent with the intuitive expectation that in order to conserve flux the excitation must on average spend equal amounts of time in the loss and gain circuits of the structure. Obviously, the reverse scenario occurs if we coupled the  $\mathcal{PT}$  dimer to the TL from the gain side.

Finally, we have experimentally studied the generalized conservation relations for the case of two-port scattering processes (see the inset of Fig. 4). Specifically, for one-

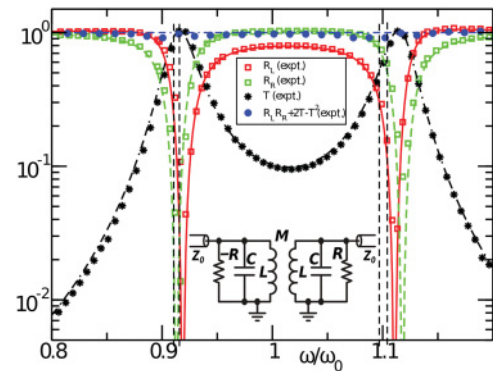


FIG. 4. (Color online) Experimental measurements (symbols) of  $T, R_{L|R}$  for the two-port scattering setup shown in the inset. The solid lines (with the corresponding colors) are the numerical values of  $T, R_{L|R}$ . The conservation relation Eq. (7)  $R_L R_R + 2T - T^2 = 1$  extracted from the experimental data is reported with blue solid circles. The horizontal dashed blue line indicates the value 1. The vertical dashed lines indicate the frequencies for which we have unidirectional transparency. We have used the same parameters as those used in Fig. 1.

dimensional (1D) geometries, it was found [13,14,19,23] that while the reflectances for left and right incident waves might be different as in the single-port case, the corresponding transmittances are the same, i.e.,  $T_L = T_R = T$ . Moreover, the following conservation relation was shown to hold [14]:

$$\sqrt{R_L R_R} = |T - 1|. \quad (7)$$

Note that Eq. (7) is an intriguing generalization of the more familiar conservation relation  $R + T = 1$ , which applies to unitary processes. In the  $\mathcal{PT}$ -symmetric case, the geometric mean of the two reflectances,  $\sqrt{R_L R_R}$  replaces the single reflectance  $R$  [26].

Our measurements for  $R_{L|R}$  and  $T$  are shown in Fig. 4. The quantity  $R_L R_R + 2T - T^2$  (blue/gray solid circles) is evaluated from the experimental data and it is found to be 1, as it is expected from Eq. (7). An interesting result of our analysis is that at specific  $\omega$  values (marked with vertical dashed lines) the transmittance becomes  $T = 1$ , while at the same time one of the reflectances vanishes. Hence, the scattering for this

direction of incidence is flux conserving and the structure is *unidirectionally transparent*. Periodic repetition of the  $\mathcal{PT}$ -symmetric unit will result in the creation of unidirectionally transparent frequency bands. The phenomenon was first predicted in Ref. [19] and its generalization was discussed in Ref. [14].

In summary, we have presented experimental evidence of the anomalous properties of  $\mathcal{PT}$ -symmetric scattering. On this basis, we propose  $\mathcal{PT}$ -symmetric *LRC* circuits as an easily realizable system where many other theoretical ideas can be investigated. Their simplicity and direct accessibility to the dynamical variables enables insight and a more thorough understanding of  $\mathcal{PT}$ -symmetric scattering. Due to space considerations, we defer a discussion of other results pertaining to the time-dependent aspects of  $\mathcal{PT}$  scattering to a subsequent publication.

We thank D. Christodoulides and V. Kovanis for useful discussions. Support from AFOSR Grant No. FA9550-10-1-0433 and NSF Grant No. ECCS-1128571 is acknowledged.

- 
- [1] C. M. Bender and S. Boettcher, *Phys. Rev. Lett.* **80**, 5243 (1998); C. M. Bender, *Rep. Prog. Phys.* **70**, 947 (2007).
  - [2] C. M. Bender, S. Boettcher, and P. N. Meisinger, *J. Math. Phys.* **40**, 2201 (1999).
  - [3] C. M. Bender, D. C. Brody, and H. F. Jones, *Phys. Rev. Lett.* **89**, 270401 (2002).
  - [4] K. G. Makris, R. El-Ganainy, D. N. Christodoulides, and Z. H. Musslimani, *Phys. Rev. Lett.* **100**, 103904 (2008).
  - [5] C. E. Rüter *et al.*, *Nat. Phys.* **6**, 192 (2010).
  - [6] Z. H. Musslimani, K. G. Makris, R. El-Ganainy, and D. N. Christodoulides, *Phys. Rev. Lett.* **100**, 030402 (2008).
  - [7] A. Guo *et al.*, *Phys. Rev. Lett.* **103**, 093902 (2009).
  - [8] L. Feng *et al.*, *Science* **333**, 729 (2011).
  - [9] H. Ramezani, T. Kottos, R. El-Ganainy, and D. N. Christodoulides, *Phys. Rev. A* **82**, 043803 (2010).
  - [10] M. C. Zheng, D. N. Christodoulides, R. Fleischmann, and T. Kottos, *Phys. Rev. A* **82**, 010103 (2010).
  - [11] S. Longhi, *Phys. Rev. Lett.* **103**, 123601 (2009).
  - [12] S. Longhi, *Phys. Rev. Lett.* **105**, 013903 (2010).
  - [13] S. Longhi, *Phys. Rev. A* **82**, 031801 (2010).
  - [14] Y. D. Chong, L. Ge, and A. D. Stone, *Phys. Rev. Lett.* **106**, 093902 (2011); L. Ge, Y. D. Chong, and A. D. Stone, *Phys. Rev. A* **85**, 023802 (2012).
  - [15] A. A. Sukhorukov, Z. Xu, and Y. S. Kivshar, *Phys. Rev. A* **82**, 043818 (2010).
  - [16] Y. D. Chong, L. Ge, H. Cao, and A. D. Stone, *Phys. Rev. Lett.* **105**, 053901 (2010).
  - [17] A. Mostafazadeh, *Phys. Rev. Lett.* **102**, 220402 (2009).
  - [18] H. Schomerus, *Phys. Rev. Lett.* **104**, 233601 (2010).
  - [19] Z. Lin *et al.*, *Phys. Rev. Lett.* **106**, 213901 (2011).
  - [20] O. Bendix, R. Fleischmann, T. Kottos, and B. Shapiro, *Phys. Rev. Lett.* **103**, 030402 (2009); C. T. West, T. Kottos, and T. Prosen, *ibid.* **104**, 054102 (2010).
  - [21] Y. N. Joglekar, D. Scott, M. Babbey, and A. Saxena, *Phys. Rev. A* **82**, 030103(R) (2010).
  - [22] J. Schindler, A. Li, M. C. Zheng, F. M. Ellis, and T. Kottos, *Phys. Rev. A* **84**, 040101(R) (2011).
  - [23] F. Cannata, J.-P. Dedonder, and A. Ventura, *Ann. Phys.* **322**, 397 (2007).
  - [24] H. J. Pain, *The Physics of Vibrations and Waves* (Wiley, Hoboken, NJ, 2005).
  - [25] The slight deviation from reciprocity in the vicinity of large reflectances in Fig. 1—see the domain around the right peak—is attributed to nonlinear effects.
  - [26] Equation (3) is a special case of Eq. (7) once we realize that in the single port case the transmittance  $T = 0$ .